ISSN 1225-8024(Print)
ISSN 2288-8403(Online)

한국표면공학회지
J. Korean Inst. Surf. Eng.
Vol. 50, No. 3, 2017.
https://doi.org/10.5695/JKISE.2017.50.3.147

<연구논문>

Electrochemical Properties of Air-Formed Oxide Film-Covered AZ31 Mg Alloy in Aqueous Solutions Containing Various Anions

Basit Raza Fazal[a,b] and Sungmo Moon[a,b,*]

[a]Surface Technology Division, Korea Institute of Materials Science, Changwon-si, Gyeongnam, Korea
[b]University of Science and Technology, Daejeon, Korea

(Received April 17, 2017 ; revised May 2, 2017 ; accepted May 2, 2017)

Abstract

This research was conducted to investigate the electrochemical properties of the thin air-formed oxide film-covered AZ31 Mg alloy. Native air-formed oxide films on AZ31 Mg alloy samples were prepared by knife-abrading method and the changes in the electrochemical properties of the air-formed oxide film were investigated in seven different electrolytes containing the following anions Cl^-, F^-, SO_4^{2-}, NO_3^-, CH_3COO^-, CO_3^{2-}, and PO_4^{3-}. It was observed from open circuit potential (OCP) transients that the potential initially decreased before gradually increasing again in the solutions containing only CO_3^{2-} or PO_4^{3-} ions, indicating the dissolution or transformation of the native air-formed oxide film into new more protective surface films. The Nyquist plots obtained from electrochemical impedance spectroscopy (EIS) showed that there was growth of new surface films with immersion time on the air-formed oxide film-covered specimens in all the electrolyte. The least resistive surface films were formed in fluoride and sulphate baths whereas the most protective film was formed in phosphate bath. The potentiodynamic polarization curves illustrated that passive behaviour of AZ31 Mg alloy under anodic polarization appears only in CO_3^{2-}, or PO_4^{3-} ions containing solutions and at more than -0.4 $V_{Ag/AgCl}$ in F^- ion containing solution.

Keywords : AZ31 Mg alloy, Air-formed oxide film, Anion effect, Corrosion resistance

1. Introduction

The importance of magnesium alloys has increased significantly in various industries due to the high strength/weight ratio, high dimensional stability, good machinability, and recyclability [1]. However, extremely negative electrode potential of magnesium makes it very active so it rapidly ionizes into Mg^{2+} ions in corrosive environments. Moreover, the hydroxide film formed on Mg alloys is less stable than passive films that form on aluminium alloys and stainless steels [2]. Therefore, poor corrosion resistance of Mg and its alloys is the major problem that has limited their widespread use in outdoor applications. Surface modification of Mg and its alloys is one of the most commonly used techniques to improve their corrosion resistance. Sol–gel-synthesized ceramic coatings [3,4], plasma electrolytic oxidation [5-11], polymer coatings [12,13], nitriding and ion implantation [14,15] chemical conversion coatings [16-18], biomimetic coatings [19,20] etc., are some of the commonly used surface modification techniques.

Electrochemical techniques such as open circuit potential (OCP) measurement, electrochemical impedance spectroscopy (EIS), and potentiodynamic polarization method are frequently used to investigate the corrosion resistance of a surface coating. Open circuit potential (OCP) measurements are carried out without application of an external current and the resulting graphs are used to determine the changes in inherent reactivity of a metal with immersion time in aqueous solutions. Electrochemical impedance spectroscopy (EIS) is a non-destructive method of performing coating evaluation in real time. EIS measurements are carried out by applying a small sinusoidal voltage at

*Corresponding Author: Sungmo Moon
Surface Technology Division, Korea Institute of Materials Science
Tel: +82-55-280-3549 ; Fax: +82-55-280-3570
E-mail: sungmo@kims.re.kr

various frequencies and measuring the current response. When an alternating potential is applied to the AZ31 Mg working electrode thin native oxide films, between the metal substrate and electrolyte, act as dielectric barrier, showing capacitive behaviour under application of the sinusoidal voltage waves. Results obtained from EIS technique are plotted in Nyquist plots or Bode plot and fitted with an equivalent electric circuit. The coating resistance and reciprocal capacitance values obtained by the fitting process are used to evaluate its corrosion protective properties and thickness of the surface films, respectively. Changes in coating resistance and reciprocal capacitance can also reveal its growth or deterioration in testing solutions [21,22]. Although EIS technique is quite useful for studying the electrochemical properties of surface oxide films on metals, still there is little published literature that deals with the changes in electrochemical properties of the air-formed oxide-covered AZ31 Mg alloy surface based on the EIS technique. Moreover, there is no literature that compares the effect of inorganic anions on the deterioration of air-formed oxide films or growth of new oxide films on AZ31 Mg alloy.

Therefore, this study is aimed at elucidating the changes in electrochemical properties of thin air-formed oxide-covered AZ31 Mg alloy upon immersion in solutions containing various anions. The air-formed oxide layer was initially produced by knife abrading method in air, and then the knife-abraded samples were tested using open-circuit potential (OCP) transient, electrochemical impedance spectroscopy (EIS) and potentiodynamic polarization methods in seven different solutions containing the following anions of Cl^-, F^-, SO_4^{2-}, NO_3^-, CH_3COO^-, CO_3^{2-} and PO_4^{3-}.

2. Experimental

2.1 Sample preparation

AZ31 Mg alloy plate (wt.%, Al 2.94, Zn 0.8, Mn 0.3, Si < 0.1, Fe < 0.005, Cu < 0.05, Ni < 0.005, and Mg balance) fabricated by POSCO was cut into 80 mm × 30 mm × 1 mm sized samples. Thin air-formed oxide film-covered samples were simply prepared by knife abrading method, so as not to form thick or porous native oxide films by contact with water [23]. The abraded sample surface was immediately covered with a masking tape to minimize surface contamination or corrosion problems. A testing area of 9 cm^2 (3 cm × 3 cm) was then drawn with an oil pen on the tape and the tape was cut along the marked lines and kept attached until used for electrochemical tests, i.e., the tape covering the test area was removed only just before the electrochemical tests.

2.2 Electrolyte preparation

Seven different electrolytes having Cl^-, F^-, SO_4^{2-}, NO_3^-, CH_3COO^-, CO_3^{2-}, and PO_4^{3-} anions were prepared using their sodium salts i.e. NaCl, NaF, $NaCH_3COO$, $NaNO_3$, Na_2SO_4, Na_2CO_3 and Na_3PO_4. Each electrolyte contains only one type of anion. Concentration of the seven different electrolytes was chosen to be 0.01 M where reaction with thin air-formed oxide film is not so fast upon immersion in the electrolytes.

2.3 Property evaluation

Open circuit potential (OCP) transients were obtained for 5 min against an Ag/AgCl reference electrode. EIS measurements and potentiodynamic polarization experiments were performed at room temperature in a three-electrode electrochemical cell, consisting of the AZ31 Mg alloy working electrode, an Ag/AgCl reference electrode, and a platinum wire mesh as the counter electrode. EIS measurement was conducted during immersion for 30 min with 5 min intervals by the application of a 10mV sinusoidal voltage in the frequency range between 100 kHz and 1 Hz. Potentiodynamic polarization curves were obtained by scanning the potential from -500 mV cathodic to +1500mV anodic versus corrosion potential at a scan rate of 5mV/s. Every electrochemical measurement was performed using Garmry Ref. 3000 instrument.

3. Results and Discussion

Figure 1 shows the OCP transients of the AZ31 Mg alloy samples immersed in solutions containing seven different anions. It can be seen that the OCP instantly

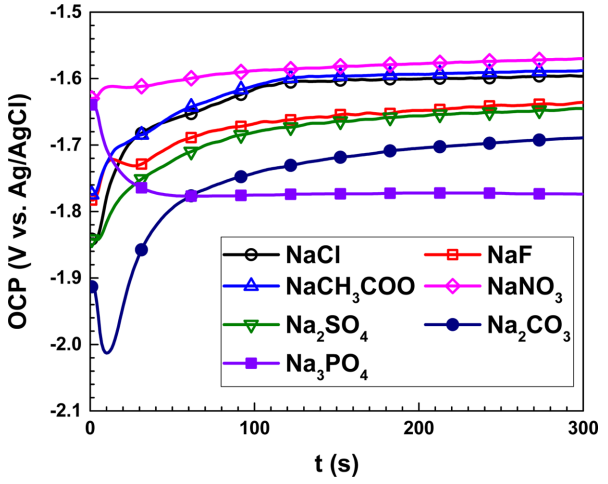

Fig. 1. Open circuit potential (OCP) transients of air-formed oxide covered AZ31 Mg alloy in 0.01 M NaCl, NaF, $NaCH_3COO$, $NaNO_3$, Na_2SO_4, Na_2CO_3 and Na_3PO_4 solutions.

increased from more active values to nobler values upon immersion in the electrolytes containing Cl^-, F^-, CH_3COO^- and SO_4^{2-} ions. The immediate increase in OCP values can be attributed to the fast formation of a new protective film on the thin air-formed oxide covered specimens. The OCP did not increase much with immersion time in a solution containing NO_{3-} anion.

In contrast, sharp drops in OCP within the first 10 ~ 30 s were observed in the CO_3^{2-} and PO_4^{3-} ion-containing solutions. The drop in potential is ascribed to dissolution of the native air-formed oxide films. The OCP value in the CO_3^{2-} and PO_4^{3-} ion-containing solutions showed fast increase immediately after the initial drop in CO_3^{2-} ion-containing solution but very slow increase after 15 min of immersion in PO_4^{3-} ion-containing solution up to 30 min.

It can also be seen from Fig. 1 that the final OCP value in the PO_4^{3-} ions bath was much more active compared to those recorded in other electrolytes. The sharp decrease in OCP within the first 30 s, the most active OCP value after 60 s of immersion, and the longest time (15 min) required for the increase in OCP in PO_4^{3-} ion-containing bath, might imply easy dissolution of the air-formed oxide film and formation of a new surface film with porous nature, allowing easy contact of the electrolyte with underlying AZ31 Mg alloy substrate.

It can be seen from Fig. 1 that nature of the thin air-formed oxide film changes within first 5 min of immersion in seven different electrolytes. It could be due to the duplex nature of the surface film on AZ31 Mg alloy which consists of a thin, nano-crystalline MgO inner layer and a $Mg(OH)_2$ outer layer [24-26]. X-ray photoelectron spectroscopy (XPS) [27-29] and focused ion beam (FIB) [26,30,31] studies on the surface of Mg have shown that the surface film, indeed, consists of both MgO and $Mg(OH)_2$ [24]. XPS and FIB have also been used to calculate the thickness of oxide layer formed on Mg and its alloys [26,30,31]. It was found that flake-like outer $Mg(OH)_2$ layer is ~500 nm thick while the inner MgO layer is only 50 - 90 nm thick [26,30,31]. This mixed layer of $MgO/Mg(OH)_2$ exhibits passive behaviour only in alkaline environments and is stable in pure alkaline solutions with pH >10.5 [32].

The instant increase of OCP values in Cl^-, F^-, CH_3COO^-, NO_3^-,and SO_4^{2-}, ions-containing solutions could be ascribed to the conversion of outer flake-like $Mg(OH)_2$ layer into $MgCl_2$, MgF_2, $Mg(CH_3COO)_2$, $Mg(NO_3)_2$ and $MgSO_4$. However, the sharp drops in OCP within the first 10 ~ 30 s in the carbonate and phosphate ions-containing solutions imply that these anions are more corrosive for the AZ31 Mg alloy substrate and can dissolve the thin nano-crystalline MgO inner layer as well before the formation and growth of $MgCO_3$ and $Mg_3(PO_4)_2$. Similar conclusions were drawn from experiments that were conducted in aerated solutions which allowed CO_2 to react with the Mg substrate and where magnesium carbonate ($MgCO_3$) was detected on the outer layer of the films [33-36].

The Nyquist plots of AZ31 Mg alloy in seven different electrolytes are shown in Fig. 2. Single capacitive loop with different diameters was obtained in the seven different solutions, which implies the presence of dielectric layers on the surface of AZ31 Mg alloy. The magnitude of the diameter was observed to increase with immersion time, indicating an increased surface film resistance due to the growth of surface oxide films.

Usually, the diameter of a capacitive loop in the Nyquist plane represents the oxide resistance and a large oxide resistance means a low corrosion rate. The oxide resistance corresponds to an ionic resistance through the oxide layer between the metal substrate and the corrosive medium. The magnitude of oxide film resistance, represented by the size of the diameter of capacitive loop, obtained from EIS data was found to be in the following order of $PO_4^{3-} > NO^{3-} > CO_3^{2-} > CH_3COO^- \sim Cl^- > F^- \sim SO_4^{2-}$.

It can also be seen from Fig. 2 that the diameter of the capacitive loop increased with increasing immersion time. The Nyquist plots obtained for the AZ31 Mg alloy sample immersed in the phosphate bath showed that initially there was a decrease in resistance before an increase in resistance after 15 min of immersion. This special behaviour in the presence of PO_4^{3-} ions also matches with the beginning of increase in OCP after 15 min of immersion. It can be assumed that the slow increase in resistance after 15 min of immersion in phosphate bath could be due to the thickening or growth of the new surface film.

To analyse the EIS spectra of the AZ31 Mg alloy sample, fitting of the data was conducted using the simple Randle's cell equivalent electrical circuit shown in Fig. 3, where R_S represents the solution resistance, R_{OX} is the oxide resistance connected in parallel to the oxide capacitance, C_{OX}. Since the Nyquist plots exhibit depressed semi-circles, a constant phase element, CPE_{OX}, replaced the C_{OX} component in the circuit.

The variation in resistance of oxide film (R_{OX}) and CPE of AZ31 Mg alloy obtained by fitting are plotted as a function of immersion time in Fig. 4. It can be seen that R_{ox} increased with immersion time in the solutions containing Cl^-, F^-, SO_4^{2-}, NO_3^-, CH_3COO^-, and CO_3^{2-} anions while it showed an initial decrease in the phosphate-ion containing bath. The increase in R_{OX} might indicate growth of the oxide film due to

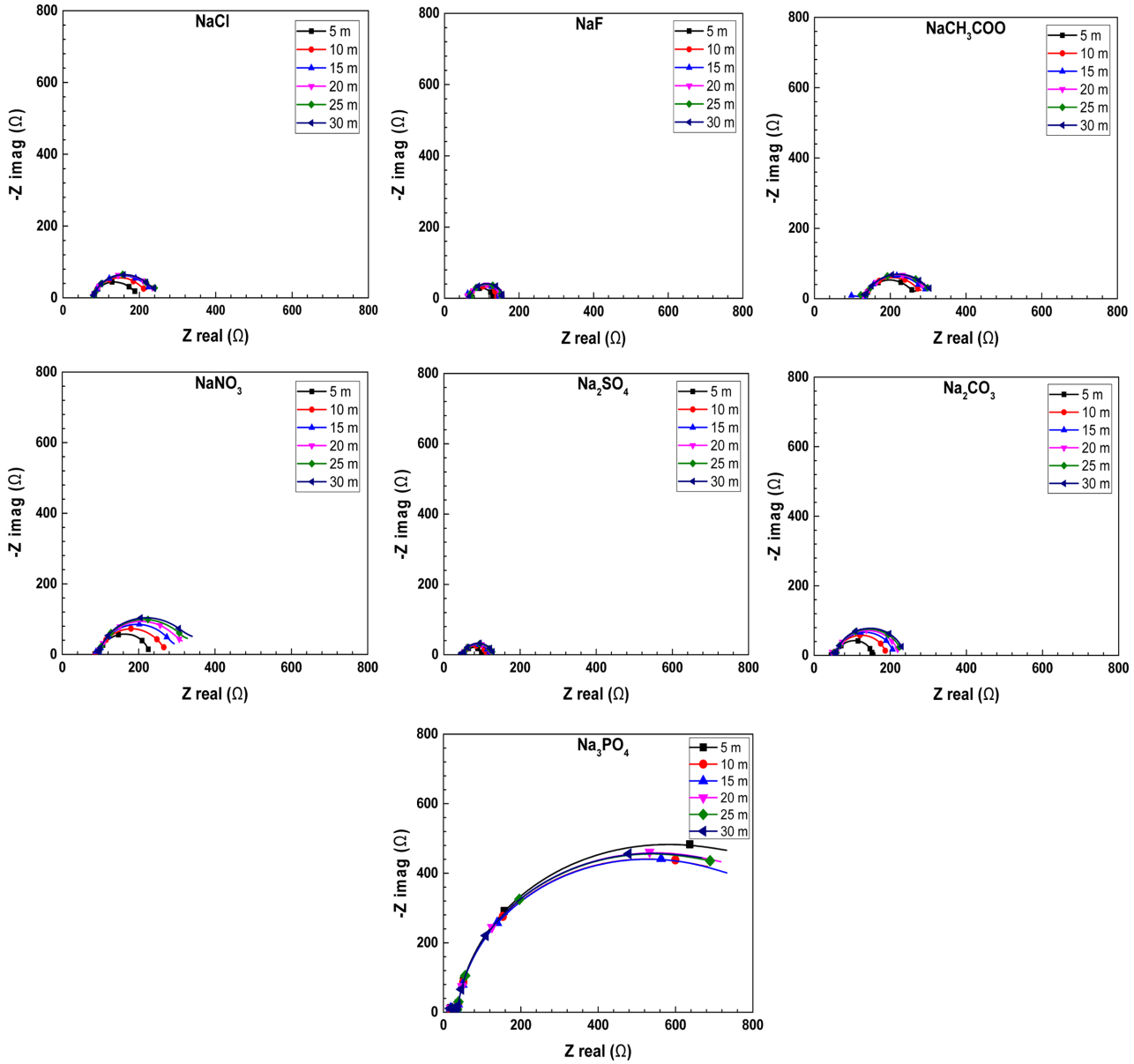

Fig. 2. Nyquist plots of AZ31 Mg alloy in 0.01 M NaCl, NaF, $NaCH_3COO$, $NaNO_3$, Na_2SO_4, Na_2CO_3 and Na_3PO_4 solutions.

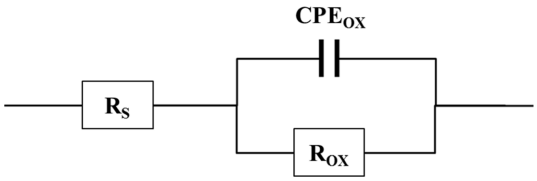

Fig. 3. Equivalent circuit used to fit EIS spectra.

the formation of a new surface layer over the air formed film on AZ31 Mg alloy substrate. On the other hand, the oxide resistance initially decreased and then increased slightly after 15 min of immersion in the phosphate-ion containing bath. The decrease in resistance could be attributed to the dissolution of the air-formed oxide film and the slight increase in resistance after 15 min could be attributed to growth of the surface film in the phosphate-ion containing bath.

The change in capacitance with immersion time is also illustrated as a function of immersion time in Fig. 4 and two distinct trends were observed. The first trend was observed in the solutions containing Cl^-, F^-, SO_4^{2-}, NO_3^-, CH_3COO^-, and CO_3^{2-} anions where the oxide capacitance decreased initially with time but slightly increased after 10 ~ 20 min. The initial decrease in capacitance could be attributed to a growth of the surface oxide film while the slight increase in capacitance can be ascribed to an increase of surface area. For example, in NaCl solution, the adsorbed chloride ions on the surface of magnesium

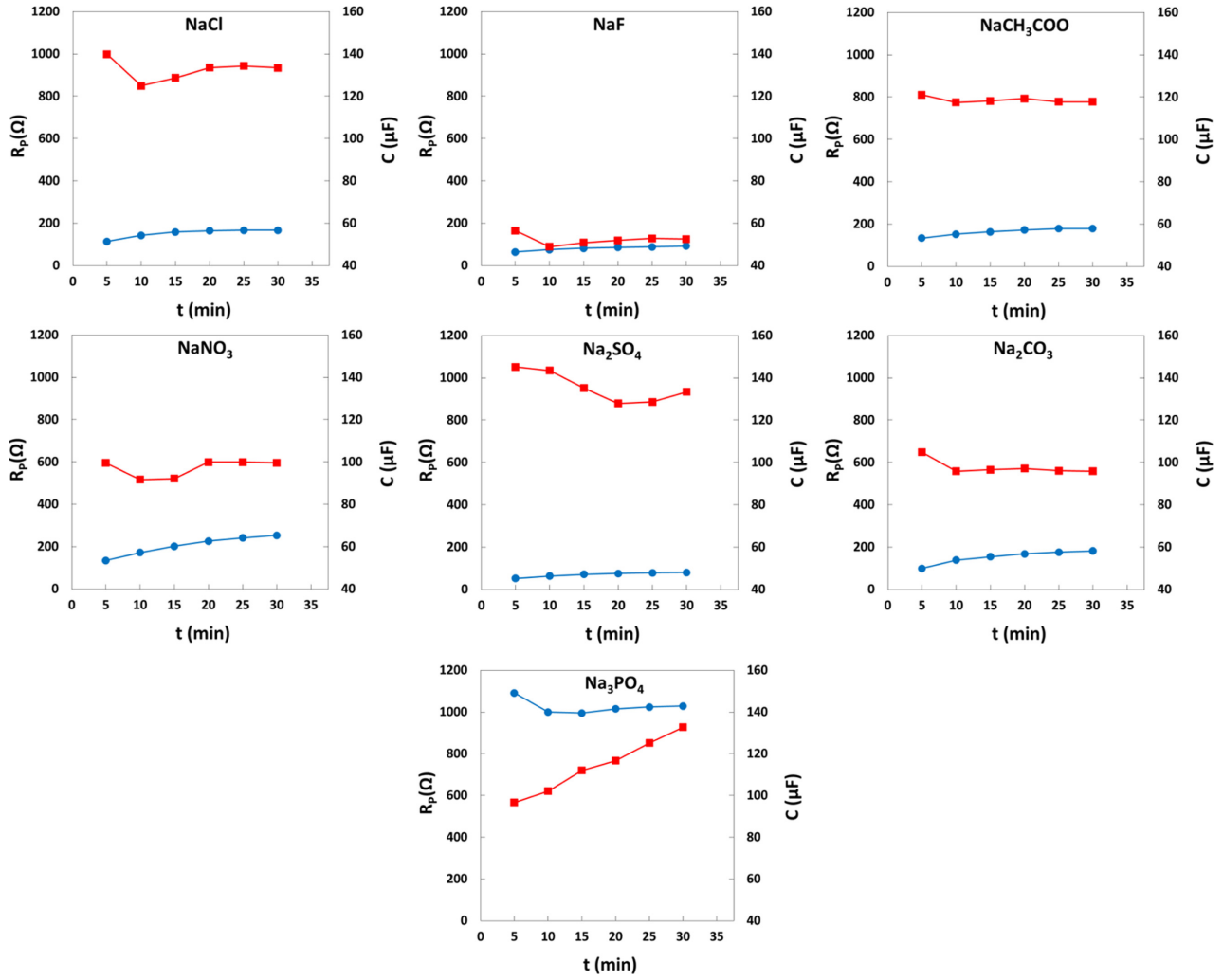

Fig. 4. Variations in resistance (●), and capacitance (■) of surface films on AZ31 Mg alloy as a function of immersion time in seven different electrolytes.

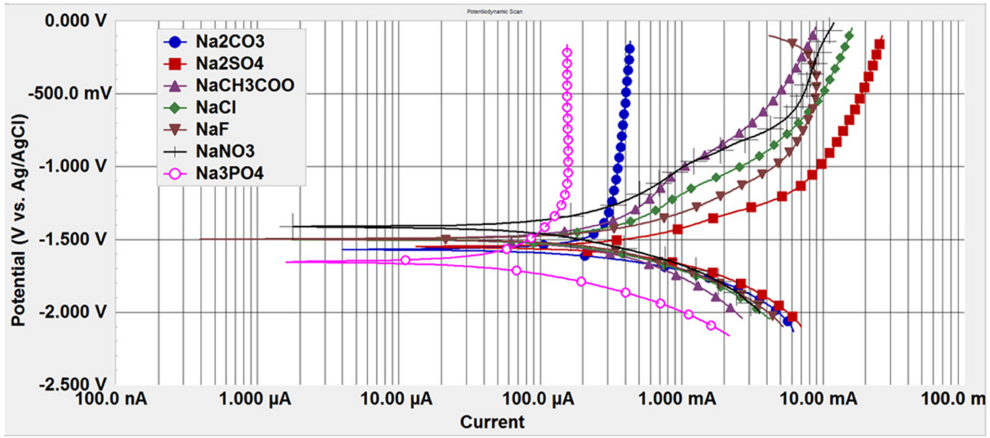

Fig. 5. Potentiodynamic polarization curves of AZ31 Mg alloy in seven different electrolytes.

alloys tend to transform $Mg(OH)_2$ into soluble $MgCl_2$ [37,38] and therefore create more film free areas where magnesium is corroded. This results in the fluctuations of capacitance but doesn't change the resistance much as one corrosion product is replaced by another [39]. The second trend was observed in the phosphate bath where the capacitance showed large increase with immersion time. The surface of the sample was found to become roughened after 30 min of immersion time due to dissolution reactions in the

phosphate bath. Thus, the large increase in oxide capacitance with time in the phosphate bath could be ascribed to an increase of surface area due to the dissolution of the substrate partly.

It can be seen from Fig.4 that after 30 min of immersion in seven electrolytes, the lowest film capacitance was obtained in fluoride ion-containing solution whereas the largest film capacitance was obtained in chloride, sulphate, and phosphate ion-containing baths. The lowest film capacitance in the fluoride bath seems to results from the smallest surface area form least surface roughening effect due to the formation of protective MgF_2 film.

Figure 5 presents the polarization curves of AZ31 obtained in the seven different electrolytes. With increasing anodic polarization, slight increase and decrease after an increase of anodic current were observed in carbonate and fluoride containing solutions, respectively. It is noted also that no increase of anodic current occurred with the increase of anodic polarization in phosphate-containing solution, suggesting the growth of porous anodic films on the AZ31 substrate. On the other hand, no passive behaviour or film growth was observed in Cl^-, SO_4^{2-}, NO_3^-, and CH_3COO^- ions-containing electrolytes.

4. Conclusions

In this work, native oxide films were prepared on AZ31 Mg alloy samples in air by knife-abrading method and changes in the electrochemical properties of those samples were examined using OCP transient, EIS and potentiodynamic polarization methods during immersion in seven different aqueous electrolytes containing various anions of Cl^-, F^-, NO_3^-, CH_3COO^-, SO_4^{2-}, CO_3^{2-} or PO_4^{3-}, and the following results were obtained.

The OCP transient of AZ31 Mg alloy samples showed initial decrease and then increase in the presence of CO_3^{2-} and PO_4^{3-} ions but it showed only increases without any initial decrease in the presence of Cl^-, F^-, NO_3^-, CH_3COO^-, SO_4^{2-} ions. These represent that the air-formed oxide film is dissolved by CO_3^{2-} and PO_4^{3-} ions and transformed into new surface. The air-formed oxide film seems to be converted into new films without its dissolution and grow in the presence of Cl^-, F^-, NO_3^-, CH_3COO^-, SO_4^{2-} ions.

The OCP transient of AZ31 Mg alloy in PO_4^{3-} ion-containing solution showed initial large decrease of about 180 mV within 1 min of immersion and very slow increase only after 15 min of immersion. The final OCP value in PO_4^{3-} ion-containing solution was also the lowest amongst the solutions containing the remaining six anions.

A single capacitive loop was obtained in Nyquist plot for all the AZ31 Mg alloy samples immersed in the seven different aqueous electrolytes. It was observed that the diameter of the capacitive loops increased with increasing immersion time in solutions of Cl^-, F^-, NO_3^-, CH_3COO^-, SO_4^{2-}, and CO_3^{2-} ions but only in the presence of PO_4^{3-} ions, there was an initial decrease and then slight increase after about 15 min of immersion. The slight increase of diameter of the capacitive loops and gradual increase in OCP after 15 min of immersion in the PO_4^{3-} ion-containing solution are attributed to the thickening of porous film; this assumption is also supported from EIS date which shows a linear increase in film capacitance with immersion time corresponding to the growth of surface film in the PO_4^{3-} ion-containing solution.

The magnitude of oxide film resistance obtained from EIS data appeared to become larger in the order of $PO_4^{3-} > NO_3^- > CO_3^{2-} > CH_3COO^- \sim Cl^- > F^- \sim SO_4^{2-}$.

Polarization curves, revealing the protectiveness of newly formed surface films, presented the lowest corrosion current density in PO_4^{3-} ion-containing solution. Passive behaviour of AZ31 Mg alloy under anodic polarization was found in CO_3^{2-} or PO_4^{3-} ion-containing solutions and in the electrolyte having F^- ions only at high anodic potentials more than -0.4 $V_{Ag/AgCl}$. The surface films formed on AZ31 Mg alloy in solutions of Cl^-, NO_3^-, CH_3COO^-, and SO_4^{2-} exhibited no passive behaviour.

Acknowledgement

This research was financially supported by a research grant from the general research program from Korea Institute of Materials Science (PNK5053).

References

[1] E. F. Emley, Principle of Magnesium Technology, Pergamon Press, London, UK, (1966).

[2] G.L. Song, A. Atrens, Corrosion Mechanisms of Magnesium Alloys, Adv. Eng. Mater. 1 (1999) 11-33.

[3] P. Amaravathy, C. Rose, S. Sathiyanarayanan and N. Rajendran, Evaluation of in vitro bioactivity and MG63oesteoblast cell response for TiO2 coated magnesium alloys, J. Sol-Gel Sci. Technol. 64 (2012) 694-703.

[4] X. Wang, S. Cai, G. Xu, X. Ye, M. Ren and K. Huang, Surface characteristics and corrosion resistance of sol gel derived CaO-P2O5-SrO-Na2O bioglass-ceramic coated Mg alloy by different heat-treatment temperatures, J. Sol-Gel Sci. Technol. 67 (2013) 629-638.

[5] T. S. N. Sankara Narayanan and M. Ho Lee, A

simple strategy to modify the porous structure of plasma electrolytic oxidation coatings on magnesium, RSC Adv. 6 (2016) 16100-16114.
[6] S. Moon and Y. Jeong, Generation mechanism of microdischarges during plasma electrolytic oxidation of Al in aqueous solutions, Corros. Sci. 51 (2009) 1506-1512.
[7] S. Moon, C. Yang, S. Na, Effects of hydroxide and silicate ions on the plasma electrolytic oxidation of AZ31 Mg alloy, J. Kor. Inst. Surf. Eng. 47 (2014) 147-154.
[8] D. Kwon, S. Moon, Effects of NaOH concentration on the structure of PEO films formed on AZ31 Mg Alloy in PO4 3- and SiO3 2- containing aqueous solution, J. Kor. Inst. Surf. Eng. 49 (2016) 46-53.
[9] S. Moon, D. Kwon, Anodic oxide films formed on AZ3 magnesium alloy by plasma electrolytic oxidation method in electrolytes containing various NaF concentrations, J. Kor. Inst. Surf. Eng. 49 (2016) 225-230.
[10] S. Moon, Y. Kim, Anodic oxidation behavior of AZ31 magnesium alloy in aqueous electrolyte containing various Na2CO3 concentrations, J. Kor. Inst. Surf. Eng. 49 (2016) 331-338.
[11] S. Moon, Corrosion behavior of PEO-treated AZ31 Mg alloy in chloride solution, J. Solid State Electrochem. 18 (2014) 341-346.
[12] J. N. Li, P. Cao, X. N. Zhang and Y. H. He, In vitro degradation and cell attachment of a PLGA coated biodegradable Mg-6Zn based alloys, J. Mater. Sci. 45 (2010) 6038-6045.
[13] A. Srinivasan, P. Ranjani and N. Rajendran, Electropolymerization of pyrrole over AZ31 Mg for biomedical applications, Electrochim. Acta, 88 (2013) 310-321.
[14] R. Xu, X. Yang, P. Li, K. W. Suen, G. Wu and P. K. Chu, Electrochemical properties and corrosion resistance of carbon ion implanted magnesium, Corros. Sci. 82 (2014) 173-179.
[15] H. M. Wong, Y. Zhao, V. Tam, S. Wu, P. K. Chu, Y. Zheng, M. K. Tsun, F. K. L. Leung, K. D. K. Luk, K. M. C. Cheung and K. W. K. Yeung, In vivo simulation of bone formation by aluminium and oxygen plasma surface-modified magnesium implants, Biomaterials. 34 (2013) 9863-9876.
[16] X. B. Chen, D. R. Nisbet, R. W. Li, P. N. Smith, T. B. Abbott, M. A. Easton, D. H. Zhang and N. Birbilis, Controlling initial biodegradation of magnesium by a biocompatible strontium phosphate conversion coatings, Acta Biomater. 10 (2014) 1463-1474.
[17] X. B. Chen, N. Birbilis and T. B. Abbott, Review of corrosion resistant conversion coatings for magnesium and its alloys, Corrosion 67 (2011) 1-16.
[18] T. Yan, L. Tan, D. Xiong, X. Liu, B. Zhang and K. Yang, Fluoride treatment and in vitro corrosion behavior of an AZ31B magnesium alloy, Mater. Sci. Eng., C, 30 (2010) 740-748.
[19] S. Shadanbaz and G. J. Dias, Calcium phosphate coatings on magnesium alloys for biomedical applications: a review, Acta Biomater. 8 (2012) 20-30.
[20] J. E. Gray-Munro, C. Seguin and M. Strong, Influence of surface modification on the in vitro corrosion rate of magnesium alloy AZ31, J. Biomed. Mater. Res., A, 91 (2009) 221-230.
[21] R.C. Bacon, J.J. Smith and F.M. Rugg, Electrolytic resistance in evaluating protective merit of coatings on metals, Ind. Eng. Chem. 40 (1948) 161-167.
[22] J.E.O. Mayne and D.J. Mills, The effect of the substrate on the electrical resistance of polymer films, J. Oil. Colour Chem. Assoc. 58 (1975) 155-159.
[23] S. Moon, A blade-abrading method for preparation of fresh surface of Mg, J. Kor. Inst. Surf. Eng. 48 (2015) 194-198.
[24] J.H. Nordlien, S. Ono, N. Masuko, Morphology and structure of oxide films formed on magnesium by exposure to air and water, J. Electrochem. Soc. 142 (1995) 3320-3322.
[25] Y. Zhu, G. Wu, Y.H. Zhang, Q. Zhao, Growth and characterization of Mg(OH)2 film on magnesium alloy AZ31, Appl. Surf. Sci. 257 (2011) 6129-6137.
[26] M. Taheri, R.C. Phillips, J.R. Kish, G.A. Botton, Analysis of the surface film formed on Mg by exposure to water using a FIB cross-section and STEM–EDS, Corros. Sci. 59 (2012) 222-228.
[27] H.B. Yao, Y. Li, A.T.S. Wee, An XPS investigation of the oxidation/corrosion of melt-spun Mg, Appl. Surf. Sci. 158 (2000) 112-119.
[28] S. Feliu, C. Maffiotte, A. Samaniego, J.C. Galvan, V. Barranco, Effect of the chemistry and structure of the native oxide surface film on the corrosion properties of commercial AZ31 and AZ61 alloys, Appl. Surf. Sci. 257 (2011) 8558-8568.
[29] S. Feliu, J.C. Galván, A. Pardo, M.C. Merino, R. Arrabal, Native air-formed oxide film and its effect on magnesium alloys corrosion, Corrosion 3 (2010) 80-91.
[30] M. Taheri, J.R. Kish, Nature of surface film formed on Mg exposed to 1 M NaOH, J. Electrochem. Soc. 160 (2013) C36-C41.
[31] R.C. Phillips, J.R. Kish, Nature of surface film

on matrix phase of Mg alloy AZ80 formed in water, Corrosion 69 (2013) 813-820.
[32] P. Kurze, Corrosion and Corrosion Protection of Magnesium, in Magnesium - Alloys and Technology, Wiley-VCH Verlag GmbH & Co. KGaA, Weinheim (2003) 218-225.
[33] M. Santamaria, F. Di Quarto, S. Zanna, P. Marcus, Initial surface film on magnesium metal: A characterization by X-ray photoelectron spectroscopy (XPS) and photocurrent spectroscopy (PCS), Electrochim. Acta 53 (2007) 1314-1324.
[34] S. Feliu Jr., M.C. Merino, R. Arrabal, A.E. Coy, E. Matykina, XPS study of the effect of aluminium on the atmospheric corrosion of AZ31 magnesium alloy, Surf. Interface Anal. 41 (2009) 143-150.
[35] S. Feliu Jr., A. Pardo, M.C. Merino, A.E. Coy, F. Viejo, R. Arrabal, Correlation between the surface chemistry and the atmospheric corrosion of AZ31, AZ80and AZ91D magnesium alloys, Appl. Surf. Sci. 255 (2009) 4102-4108.
[36] R. Lindström, L.G. Johansson, G.E. Thompson, P. Skeldon, J.E. Svensson, Corrosion of magnesium in humid air, Corros. Sci. 46 (2004) 1141-1158.
[37] L. Wang, T. Shinohara, B.P. Zhang, Influence of chloride, sulphate and bicarbonate anions on the corrosion behaviour of AZ31 magnesium alloy, J. Alloys Compd. 496 (2010) 500-507.
[38] S. Feliu Jr., C. Maffiotte, J.C. Galvan, V. Barranco, Atmospheric corrosion of magnesium alloys AZ31 and AZ61 under continuous condensation conditions, Corros. Sci. 53 (2011) 1865-1872.
[39] S.A. Salman, R. Ichino, M. Okido, A Comparative Electrochemical Study of AZ31 and AZ91 Magnesium Alloy, Int. J. Corros. (2010) 1-7.